Mon. Not. R. Astron. Soc. **395,** 531–536 (2009) doi:10.1111/j.1365-2966.2009.14574.x

Correcting CCD photometry of stars for seeing effects

Chris Koen★

Department of Statistics, University of the Western Cape, Private Bag X17, Bellville, 7535 Cape, South Africa

Accepted 2009 January 29. Received 2008 December 8; in original form 2008 September 25

ABSTRACT

Systematic variability in stellar magnitudes, as derived from profile fitting to CCD images, may in some instances be due to variable seeing. It is suggested that this happens in cases where the stars are unresolved pairs, typically with sub-arcsecond separation between the components. It is shown that the fitting of suitable Generalised Additive Models to time series photometry can disentangle intrinsic stellar variability and seeing-induced brightness changes. It is possible that there will be a fixed seeing response associated with a given star which exhibits the effect: estimation of this response from several long photometric runs is demonstrated.

Key words: methods: data analysis – techniques: photometric.

1 INTRODUCTION

Fig. 1 shows time series photometry of five stars from a sparsely populated field, obtained by fitting Gaussian profiles to CCD images. The measurements have been differentially corrected with respect to the two brightest stars in the field of view. Clearly most stars are non-variable, but the light curve in panel 3 suggests that star is an irregular variable.

In Fig. 2, the same magnitudes are plotted against a measure of seeing (see point 4 below), rather than against time. The very good correlation ($r = -0.88$) between seeing and the brightness of star 3 explains the apparent variability in Fig. 1.

Inadequate flat-fielding, or poor pixels, can be ruled out as the explanation for this effect, since it is seen consistently for the same star on different nights, despite the images being located at different positions on the CCD frame. A clue as to the likely origin comes from the literature on three objects in which brightness–seeing correlations have been observed, namely Kelu 1, ϵ Indi B and 2MASS 0746425+2000321AB (2M 0746+2000AB). Each of these is a very close pair, of similar brightness, which is usually unresolvable by conventional photometry. Both Kelu 1 and 2M 0746+2000AB comprise two very similar early L components, with separations 0.29 and 0.22 arcsec, respectively (Reid et al. 2001; Liu & Leggett 2005). The determinations were made using an adaptive optics system and by *Hubble Space Telescope*, respectively. Similarly, McCaughrean et al. (2004) used adaptive optics to confirm the finding by Volk et al. (2003) that ϵ Indi B is a T1+T6 binary. The angular separation of the two components is 0.73 arcsec.

The following then seems plausible: since the images of the two components of the pair are always unresolved, the CCD reduction software treats it as a single star. Under good seeing conditions, the profile will nonetheless deviate from that of a single object, and the reductions will miss some of the light (i.e. there will be considerable positive residuals). The poorer the seeing, the more the two components will be blended, and the better the profile fit will be. This implies that the reductions will be better at capturing the full flux when the seeing is poor.

Section 2 describes simulation results supporting the notion that profile-derived fluxes of blended images increase with poorer seeing. Sections 3 (single runs) and 4 (repeated runs) deal with the methodology of deducing seeing corrections, and Section 5 remarks on a few avenues to be explored in further studies.

A few remarks that need to be made are as follows.

(1) All the photometric reductions discussed in this paper were performed with DOPHOT (Schechter, Mateo & Saha 1993). It is likely that other reduction software will not precisely show the same effects. It seems more plausible, though, that only the level of the effect will depend on the software.

(2) Following on from point 1, the relative merits of different CCD reduction packages are not an issue here (see Becker et al. 2008 for a critical assessment). The DOPHOT software continues to be widely used – the SAO/NASA Astrophysics Data System notes 112 references to the Schechter et al. (1993) paper for the period 2004–2007. Reductions with DOPHOT of very low-amplitude (typically smaller than 5 mmag) variable stars have in any case convincingly demonstrated that high-accuracy profile-fitted magnitudes can be obtained with this software (e.g. Stobie et al. 1997; Koen et al. 1999).

(3) Also, left aside is discussion of the accuracy of fluxes found by profile fitting versus those obtained by aperture photometry. Though information in the literature appears to be scarce, careful studies suggest that aperture photometry of single stars may be more accurate, if meticulously performed (O'Donoghue et al. 2000; Tuvikene et al. 2007).

(4) The primary measure of seeing used in this paper is the standard deviation σ of the Gaussian profile, measured in pixels. The equivalent full width at half-maximum can be obtained by multiplication by 2.35. Observational data shown were obtained with

★E-mail: ckoen@uwc.ac.za

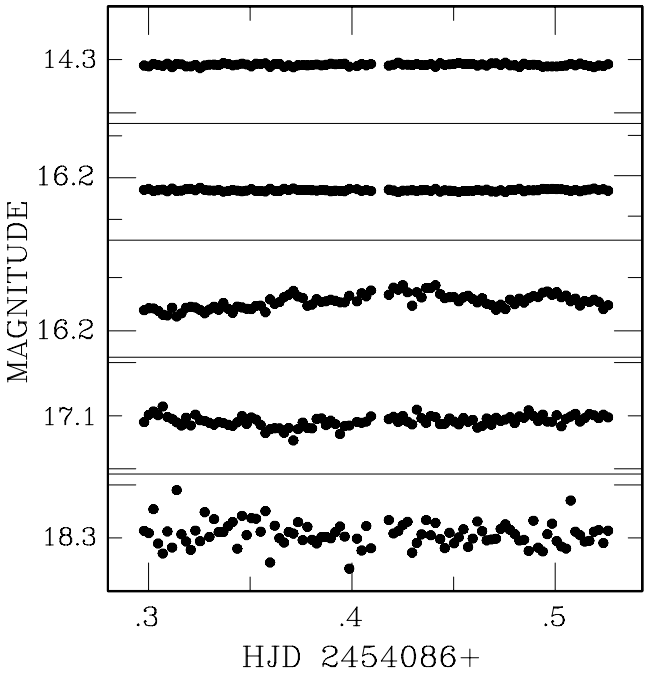

Figure 1. Differential CCD time series photometry of a star field. The tick marks on the vertical axis are 0.1 mag apart; each panel has height 0.22 mag. There is apparently systematic variability, with an amplitude of about 0.1 mag, in the light curve plotted in the central panel. Note that this star is of comparable brightness to that in the second panel.

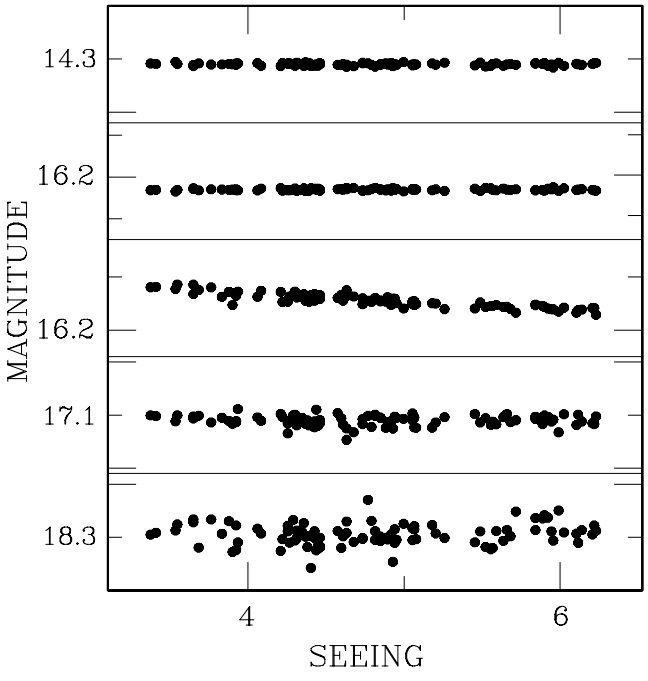

Figure 2. As for Fig. 1, but magnitudes are plotted against seeing rather than time.

the South African Astronomical Observatory 1.9-m telescope: its pixel scale can be converted to arcseconds by multiplication by 0.29 arcsec pixel^{-1}.

(5) For completeness, it is noted that all the actual photometric data shown in the paper were obtained in the I_C band.

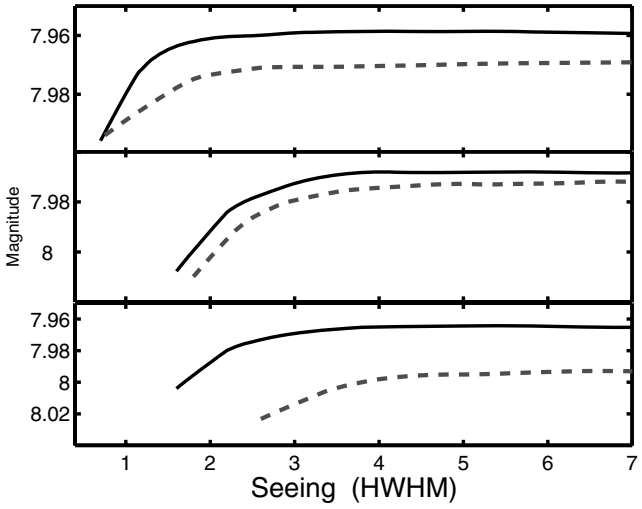

Figure 3. Profile magnitudes estimated from simulated equal-magnitude unresolved pairs with separations 1 pixel (top panel), 2 pixels (middle panel) and 3 pixels (bottom panel). The horizontal axis gives the simulated seeing. The experiment was performed twice, for two different magnitude levels: the results for the fainter, for which zero-points have been shifted, are shown by the broken lines.

2 SIMULATION EXPERIMENTS

Simulations were done with the IRAF package ARTDATA, using the command MKOBJECTS. The simulated stellar images were added to a low-illumination frame, which had been obtained with a long exposure, with the telescope mirror cover closed. Each frame contained 33 Moffat-profile images, nine of which were used as local standards. Two of the remaining stellar images were single, and used as checks on the results. Close doubles were simulated at separations of 0.5, 1, 1.5, 2, 2.5, 3, 4, 5 and 10 pixels. Each component of the double had the same brightness; a second set of doubles, with the same separations but 1 mag brighter, was also simulated. Only round images were simulated, with half-intensity radii ranging from 0.5 to 8.4 pixels ($0.42 \leq \sigma \leq 7.1$ pixels); the 'exposure time' parameter was increased for larger images. The Poisson noise was added to each of the simulated images.

The sole aim of the simulation exercise was to investigate the conjecture that the calculated magnitudes are seeing-dependent. Therefore, no attempt was made to optimize the reductions, or to explore many simulation configurations. Furthermore, a single simulation of each radius size was performed – a thorough study would require the calculation of average results over many simulations.

The reduction software always correctly identified both components in the two cases of widest separation (5 and 10 pixels). For smaller closer separations, both components could only be found for better seeing values. As an example, for half width at half-maximum seeing in excess of 2.5 ($\sigma > 2.1$), all 'stars' with separation less than 4 pixels were identified as single – which is perhaps not surprising.

Illustrative results can be seen in Fig. 3, which is based on the DOPHOT profile magnitudes of unresolved doubles treated as single. The figure shows smooth local linear fits to the simulated data. The seeing dependence of the brightness determinations is clear.

3 ESTIMATING THE SEEING EFFECT FROM REAL DATA

The fact that measured brightnesses may vary in time due to both intrinsic stellar variations and changing seeing poses a challenge,

since the functional forms of both the time and the seeing dependence of the variations may be unknown. This suggests a general non-parametric regression of the form

$$m(t, s) = \alpha + f_t(t) + f_s(s) + e(t, s), \quad (1)$$

where m, the magnitude measure, depends on both time t and seeing s, through the zero-mean functions f_t and f_s, respectively. The zero-point is given by the constant α, and e is the residual. The forms of f_t and f_s are left unspecified, since they are unknown: they are to be derived from the data.

Equation (1) is of the form of a 'Generalised Additive Model' (GAM) (see e.g. Hastie & Tibshirani 1990). Comparison of (1) to the multiple linear regression equation

$$m(t, s) = \alpha + At + Bs + e(t, s)$$

(A and B being constants) shows that GAMs considerably extend the range of ordinary regression models. Although the additive form of (1) assumes that the effects of time t and s are independent, interactions can also be catered for by, e.g., introducing a function of ts.

It is necessary to place some restrictions on the functions, f_t and f_s, in order to get sensible results. The most important of these is the requirement that the functions should be smooth: the underlying philosophy is that irregularities in the data will primarily be due to the noise term, and therefore should not be modelled by f_t and f_s. The quantity

$$\int [f''(x)]^2 \, \mathrm{d}x$$

is a typical measure of 'smoothness'. Models are fitted by 'penalized maximum likelihood' methods – the Gaussian likelihood of the model is maximized, subject to a penalty term for the degree of non-smoothness of the estimated f_t and f_s. The penalty term is taken proportional to a 'smoothing constant', which is estimated separately by cross-validation. (In cross-validation, data points are left out one at a time, and the accuracy with which a model fitted to the remaining data is then assessed. The optimal smoothing constant is the one which leads to the best overall prediction accuracy).

Considerable detail is available in e.g. Hastie & Tibshirani (1990) and Wood (2006). A brief discussion of the estimation of α, and the functions f, can also be found in Koen & Lombard (2007), who describe an astronomical application. The calculations reported below were performed with the R software package MGCV (Wood 2006) which is very convenient to use (e.g. Koen, Kanbur & Ngeow 2007).

The functions, f_t and f_s, fitted to the data in the middle panel of Fig. 1, are plotted in Figs 4 and 5. The amplitude of the time variability as given by f_t is almost an order of magnitude smaller than that shown in Fig. 1, while the seeing variability is considerable. The result is not surprising: comparison of Figs 1 and 2 indicates that seeing is a much better predictor of the star's brightness than time. Given the relatively wide confidence envelope for f_t, it seems reasonable to conclude that there is, in fact, little evidence for *any* time variability in the star.

A second example, for the close pair 2M 0746+2000AB, can be seen in Figs 6 and 7. Here, there is much stronger evidence for intrinsic variability of the system, but the seeing-induced component is again somewhat larger.

4 ESTIMATION OF THE SEEING EFFECT FROM REPEATED RUNS

It is, of course, unlikely that exactly the same estimated form of f_s will be obtained for different runs on the same object, particularly if it is also intrinsically variable. Figs 8–10 show estimated seeing functions for three ultracool (i.e. spectral types later than M8) systems, each of which has been the subject of a number of observing runs. Although there is broad agreement between the curves for a given object, there may also be considerable variation (e.g. Fig. 8). In order to proceed, the assumption is made that the variation in shape of the f_s from different runs is a sampling effect, i.e. it is postulated that there is some fixed underlying form of f_s, say F_s. The aim of this section of the paper is the estimation of F_s from the collection of individual f_s.

The basic idea is the following: the total seeing interval covered by all the runs is divided into I equally wide sub-intervals, indexed by i ($i = 1, 2, \ldots, I$). The values of the f_s in each of these bins are then averaged to estimate the $F_s(i)$. Of course, the fly in the ointment is that the zero-points of the individual f_s are arbitrary, in the sense that the mean f_s is zero for each run. It is therefore necessary to obtain a zero-point for each run: this is done by minimizing the scatter in each seeing bin, summed over all bins.

Since any given run may only cover a restricted seeing interval, only function values corresponding to measured values of the seeing

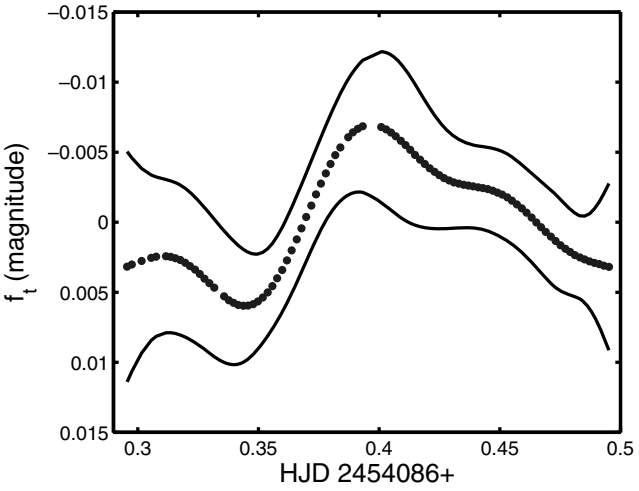

Figure 4. The function f_t (dots) for the data in panel 3 of Fig. 1. The solid lines indicate the ±2 standard error limits for each point estimate.

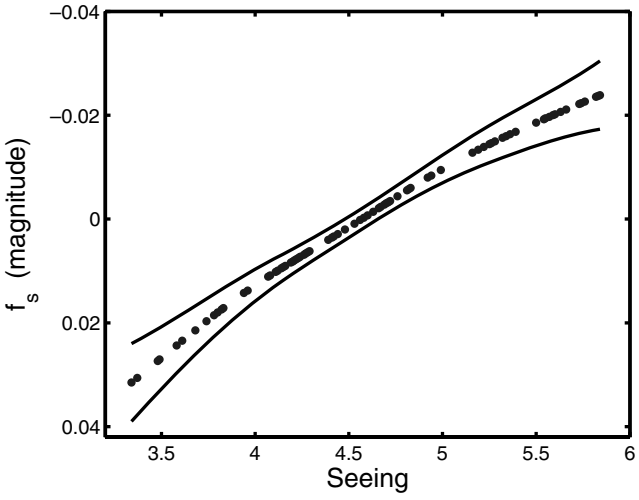

Figure 5. The function f_s (dots) for the data in panel 3 of Fig. 1. The solid lines indicate the ±2 standard error limits for each point estimate.

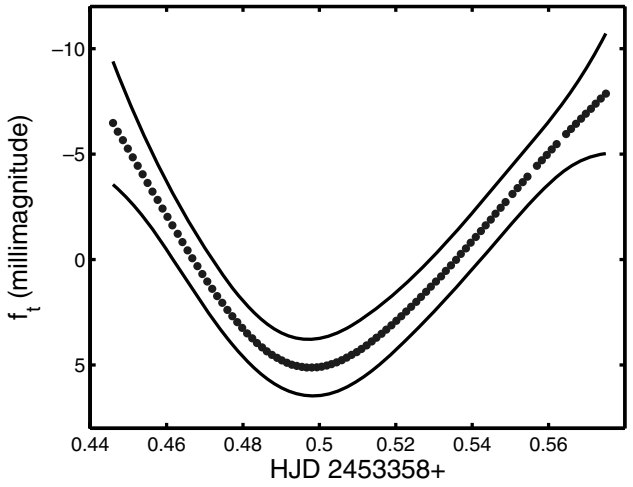

Figure 6. The function f_t (dots) for a run on the ultracool system 2M 0746+2000AB. The solid lines indicate the ± 2 standard error limits for each point estimate.

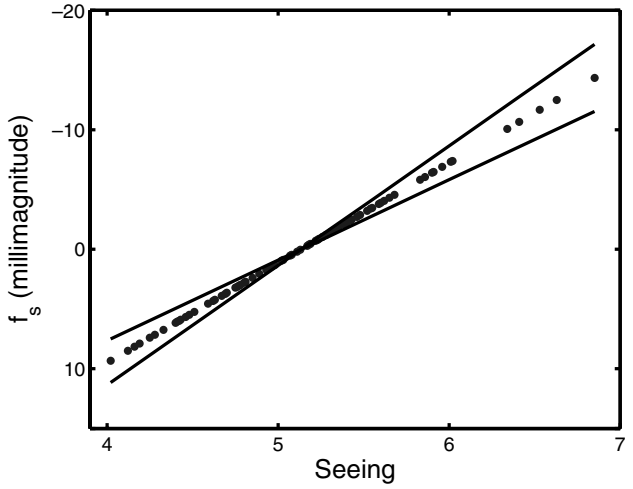

Figure 7. The function f_s (dots) for a run on the ultracool system 2M 0746+2000AB. The solid lines indicate the ± 2 standard error limits for each point estimate.

are used. Let f_{sk} be the seeing function from run number k ($k = 1, 2, \ldots, K$), and let its unknown offset be z_k. Denote by n_{ki} the number of seeing measurements from run k which lie in seeing interval i. The zero-points z_k are determined by minimization of

$$SS = \sum_{i=1}^{I} \sum_{k=1}^{K} \sum_{j=1}^{n_{ki}} \{[f_{sk}(s_{kij}) + z_k] - F_s(i)\}^2, \tag{2}$$

where the bin averages $F_s(i)$ are given by

$$F_s(i) = \sum_{k=1}^{K} \sum_{j=1}^{n_{ki}} [f_{sk}(s_{kij}) + z_k] \Bigg/ \sum_{k=1}^{K} n_{ki}. \tag{3}$$

Of course, more sophisticated schemes involving different widths for the seeing intervals and weighting of the terms in (2) could be devised, but given the nature of the data this does not seem warranted.

The results of applying the above simple method, with $I = 40$, are plotted in Fig. 11 (results obtained with $20 \leq I \leq 50$ are all very

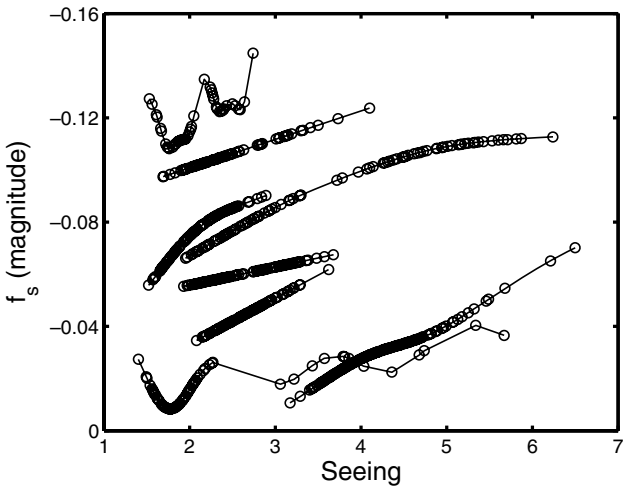

Figure 8. Estimated functions f_s for eight different runs on Kelu-1. The magnitude zero-points are arbitrary.

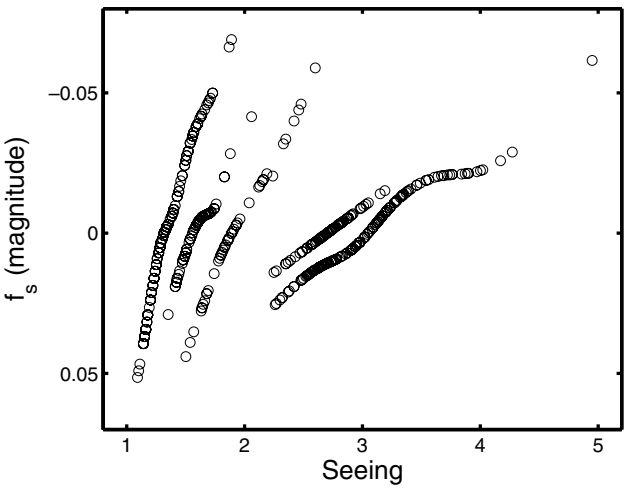

Figure 9. Estimated functions f_s for five different runs on ϵ Indi B. The magnitude zero-points are arbitrary.

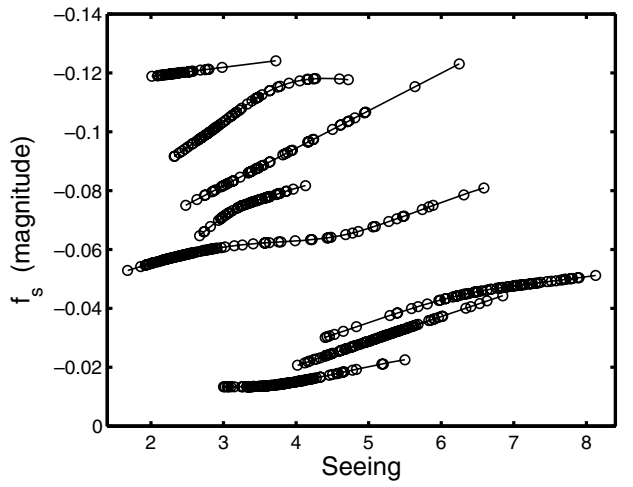

Figure 10. Estimated functions f_s for eight different runs on 2M 0746+2000AB. The magnitude zero-points are arbitrary.

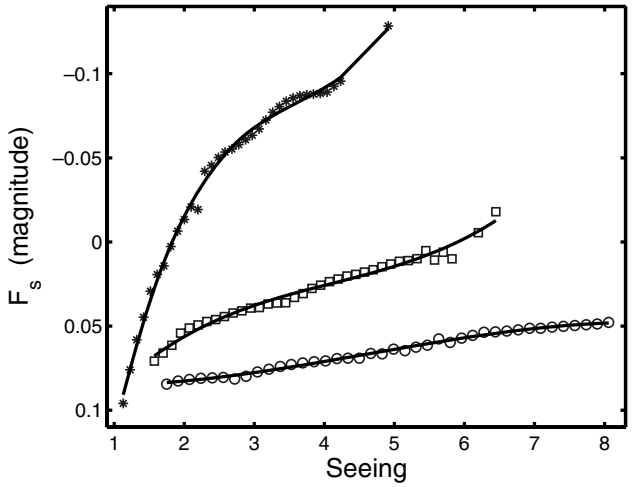

Figure 11. Estimated functions F_s for ϵ Indi B (asterisks), Kelu-1 (squares) and 2M 0746+2000AB (circles). The solid lines are third-order polynomial fits. The magnitude zero-points are arbitrary.

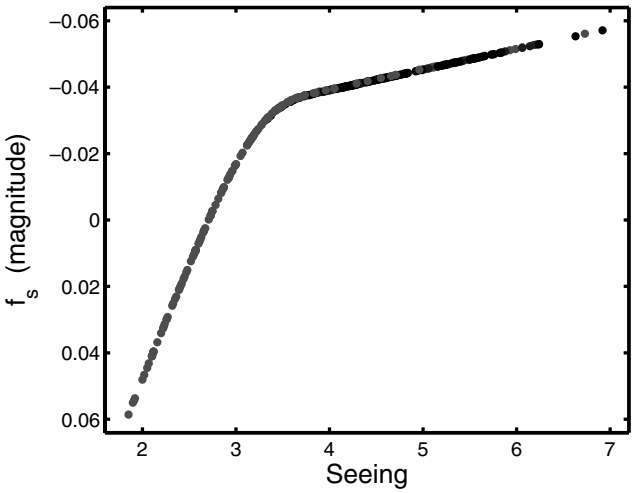

Figure 12. Estimated functions f_s for five different sets of measurements of a star in the field of DENIS-P J0255-4700. The magnitude zero-points have been adjusted to best align the functions.

similar). Comparison of the three curves shows that the magnitude of the seeing effect is largest for the system with the largest separation (ϵ Indi B) and smallest for the closest pair (2M 0746+2000AB), in agreement with expectations. The polynomial fits to the results can now conveniently be used to correct the photometry for the seeing effects.

A more accurate view is afforded by results for a star in the field of DENIS-P J0255-4700 (at α = 02:54:59.4, $\delta = -47$:02:50.2; $I = 15.8$). For reasons which probably include good differential corrections, and no intrinsic stellar variability, the functions f_s from different runs agree extremely well. Slight zero-point adjustments were made to obtain the graph in Fig. 12, but no averaging over the different f_s has been performed: the five individual seeing functions are simply plotted together. The position and shape of the bend in the curve (at seeing $\sim$3) agree quite well with the similar feature in the ϵ Indi B F_s plot (Fig. 11).

5 FURTHER WORK

(1) The simulations performed were simple, but perhaps not very realistic. In particular, the simulated magnitude seeing plots reach a plateau for relatively small values of seeing, in disagreement with what is found in the observed data.

(2) The performance of other reduction packages on seeing-affected data has not been tested. For completely unresolved star images, it is not obvious that these would necessarily fare better, but this should be investigated. If substantially superior results are obtained with other software, then clearly DOPHOT should be used with circumspection.

(3) If the angular separation between the two objects is known (from e.g. space-based photometry), then two profiles with this separation could be fitted to the single unresolved image. In theory, this should provide accurate photometry.

(4) In principle, the effect discussed in this paper could be used to identify close pairs with similar brightness, from unresolved images. This could be done by taking a succession of exposures with different telescope focus settings under constant seeing conditions, and studying differential brightnesses derived from profile fitting.

(5) It seems likely that the detailed forms of graphs, such as those in Figs 11 and 12, should depend only on the separation between, and relative brightnesses of, the two components. It may therefore be possible to calibrate such graphs using information for pairs which have been resolved by other means (interferometry, adaptive optics and/or space-based photometry) or, alternatively, by computer-generated images.

(6) If the estimated seeing function $f_s(s)$ is close to linear (e.g. Figs 5 and 7), then equation (1) could be replaced by

$$m(t, s) = \alpha + f_t(t) + \beta s + e(t, s), \tag{4}$$

where the slope β is fixed, but unknown. Estimation of β can be performed more efficiently than estimation of an unknown $f_s(s)$, and hence superior estimates of $f_t(t)$ will be obtainable from equation (4).

ACKNOWLEDGMENTS

The author is grateful for the efforts of those who have developed and maintained the IRAF and R software packages.

REFERENCES

Becker A. C., Silvestri N. M., Owen R. E., Ivezić Ž., Lupton R. H., 2007, PASP, 119, 1462
Hastie T. J., Tibshirani R. J., 1990, Generalised Additive Models. Chapman & Hall, London
Koen C., Lombard F., 2007, MNRAS, 382, 693
Koen C., O'Donoghue D., Kilkenny D., Stobie R. S., Saffer R. A., 1999, MNRAS, 306, 213
Koen C., Kanbur S., Ngeow C., 2007, MNRAS, 380, 1440
Liu M. C., Leggett S. K., 2005, ApJ, 634, 616
McCaughrean M. J., Close L. M., Scholz R.-D., Lenzen R., Biller B., Brandner W., Hartung M., Lodieu N., 2004, A&A, 413, 1029
O'Donoghue D., Kanaan A., Kleinman S. J., Krzesinski J., Pritchet C., 2000, Balt. Astron., 9, 375
Reid I. N., Gizis J. E., Kirkpatrick J. D., Koerner D. W., 2001, AJ, 121, 489
Schechter P. L., Mateo M., Saha A., 1993, PASP, 105, 1342
Stobie R. S., Kawaler S. D., Kilkenny D., O'Donoghue D., Koen C., 1997, MNRAS, 285, 651

Tuvikene T., Bouzid M. Y., Ederoclite A., Sterken C., 2007, in Sterken C., ed., ASP Conf. Ser. Vol. 364, The Future of Photometric, Spectrophotometric and Polarimetric Standardization. Astron. Soc. Pac., San Francisco, p. 579

Volk K., Blum R., Walker G., Puxley P., 2003, Int. Astron. Union Circ., 8188

Wood S., 2006, Generalized Additive Models. An Introduction with R. Chapman & Hall/CRC, Boca Raton, Florida

This paper has been typeset from a TEX/LATEX file prepared by the author.